

## Theory of pinned fronts

Haim Weissmann, Nadav M. Shnerb, and David A. Kessler

*Department of Physics, Bar-Ilan University, Ramat-Gan IL52900, Israel*

(Received 13 August 2015; revised manuscript received 16 November 2015; published 11 January 2016)

The properties of a front between two different phases in the presence of a smoothly inhomogeneous external field that takes its critical value at the crossing point is analyzed. Two generic scenarios are studied. In the first, the system admits a bistable solution and the external field governs the rate in which one phase invades the other. The second mechanism corresponds to a continuous transition that, in the case of reactive systems, takes the form of a transcritical bifurcation at the crossing point. We solve for the front shape and for the response of competitive fronts to external noise, showing that static properties and also some of the dynamical features cannot discriminate between the two scenarios. A reliable indicator turns out to be the fluctuation statistics. These take a Gaussian form in the bifurcation case and a double-peaked shape in a bistable system. Our results are discussed in the context of biological processes, such as species and communities dynamics in the presence of a resource gradient.

DOI: [10.1103/PhysRevE.93.012405](https://doi.org/10.1103/PhysRevE.93.012405)

### I. INTRODUCTION

Front propagation is one of the well-studied aspects of nonlinear physics. When a spatial system undergoes a phase transition one should not expect, in general, a global response of the system to a change of an external parameter. Rather, in a typical scenario a nucleus of the new phase appears, either within the system or at its edge, and spreads to fill it. In most cases this spreading process involves the propagation of a front between the two phases.

Two main types of fronts are considered in the literature [1]. When a first-order transition occurs, the stable phase propagates into a metastable state. For example, below 0°C both water and ice are local minima of the free-energy function, but the ice minimum is global, hence a (sufficiently large) ice droplet will invade the water. In this case the invasion front belongs to the Ginzburg-Landau (GL) class and its minimal model is given by the equation ( $\phi$  is the local fraction of one of the phases,  $\phi = 1$  and  $\phi = 0$  are the stable fixed points)

$$\dot{\phi}(x,t) = D\nabla^2\phi(x,t) + \phi(x,t)[1 - \phi(x,t)][\phi(x,t) - C]. \quad (1)$$

The velocity of the front is determined by the energy difference between the corresponding minima and it has a stall (i.e., Maxwell, or melting) point at the transition ( $C = 1/2$ ), where its velocity vanishes.

The other prototype of front propagation is the Fisher front [1,2], which characterizes the invasion of a stable state into an *unstable* one. The generic mathematical description of these fronts is given by the celebrated Fisher-KPP equation,

$$\dot{a}(x,t) = \nabla^2 a(x,t) + C[a(x,t) - a^2(x,t)], \quad (2)$$

where  $a(x,t)$  is the concentration of the invading “reactant” (chemical, protein, species). The process described by Fisher-KPP equation—logistic growth with diffusion—is inherently out-of-equilibrium; still it carries some similarities to second-order transitions, since the transcritical bifurcation at  $C = 0$  is continuous.

Despite the extensive study of phase transitions and front propagation in many natural systems, relatively little attention has been given to the properties of static fronts, trapped by a smooth, spatial gradient of an external field. This is

a very common scenario: it appears in junctions between different materials, under temperature and magnetic field spatial gradients, when birth-death-dispersal processes of animals or pathogens takes place in varying environments and so on. However, only recently has the equilibrium properties of thermodynamic systems with a spatially varying temperature that takes its critical value in a localized region begun to be studied [3].

Here we present a study of the properties of out-of-equilibrium pinned fronts, i.e., we consider the case where  $C$  [in Eqs. (1) and (2)] is  $x$  dependent, such that one phase is preferred for  $x > 0$  and the other phase is preferred for  $x < 0$ , assuming that the gradient of  $C(x)$  is slow (with respect to the other relevant length scales defined below). Static properties, such as the shape of the front, and dynamic properties, such as the fluctuation statistics under noise, are calculated.

Motivated by recent studies of the dynamics of ecological and biological systems [4–6], our main interest is in developing the ability to infer the characteristics of the underlying process from the properties of the pinned front. As will be explained in detail in the discussion section, the distinction between bistable, Ginzburg-Landau systems, which support discontinuous transitions and catastrophic shifts [7], and Fisher-like systems in which the transition between states is continuous, plays a crucial role in many fields of biological sciences (see, for example, Refs. [6,8,9]). In this context, we provide two main results: first, we show that the static shape of the front is very similar in both scenarios, so under a reasonable level of measurement accuracy and noise one cannot use it to infer the underlying dynamics unless one can systematically vary, or measure the system parameters. On the other hand, we show that the fluctuation statistics differ qualitatively between GL and Fisher systems, thus suggesting it as a reliable diagnostic tool.

In the context of biology or ecology, Eqs. (1) and (2) describe single species dynamics, for which  $C(x)$  represent an abiotic external field that sets the range limits of the species. Many recent works, in particular those focused on regime shifts and catastrophic transitions, adopt an alternative approach, assuming that the fronts are competitive, i.e., that two species A and B are competing with each other, where the

spatially varying abiotic field affects the relative fitness of the competitors, causing A to select out B in one spatial region and B to win in a different location. Following these approaches, we implement, throughout this paper, models of competitive fronts that will be presented in the next section. However, almost all our main results are relevant to both single species and competitive fronts. The distinction between competitive and abiotic fronts, including the possibility of a mixed front, is discussed in more detail in Sec. IV.

This paper is organized as follows. In the next section we present the two models for competitive fronts, explaining the differences between them. Section III is devoted to the analysis of the static properties of these models, while in Secs. IV and V their dynamic features are discussed. In Sec. VI we discuss the relationships between the out-of-equilibrium GL model and the equilibrium pinned front considered in Ref. [3]. Finally, in the last section the applicability of our results is discussed, both in general and with respect to a few recent empirical studies.

## II. TWO MODELS OF PINNED, COMPETITIVE FRONTS

In this section we would like to present the competitive front version of Eqs. (1) and (2), and to consider both our models, side by side, in order to emphasize the similarities and dissimilarities between them and to discuss in more detail their features and their practical relevance.

To model a competitive front we consider two species along a one-dimensional line, their local densities being given by  $a(x,t)$  and  $b(x,t)$ . These species compete with each other, such that the deterministic solution of a well-mixed scenario is either pure  $a$  or pure  $b$ . However, an external inhomogeneous field  $C(x)$  makes  $a$  fittest for  $x < 0$  while  $b$  is the fittest for  $x > 0$ .  $C(x)$  is a measure of the relative advantage of a species, such that when  $C = 0$  both species admit the same fitness. If  $C(x) = \tanh(x/x_t)$ , for example,  $x_t$  determines the width of the transition region (which is not necessarily equal to the front width, as we shall see below).

Let us begin with the bistable model, for which Eq. (1) is the standard single-species analog. To construct a simple two-species generalization of Eq. (1), we define  $S(x,t) = a(x,t) + b(x,t)$  and  $Q(x,t) = a(x,t) - b(x,t)$ , both species diffuse with the same diffusion constant  $D$ , and their local dynamics satisfies

$$\dot{S} = S(1 - S) \quad \dot{Q} = (Q - C(x))(S^2 - Q^2), \quad (3)$$

so that the stable fixed points correspond to  $S = 1$  and  $Q = \pm 1$ , meaning that either  $a = 1, b = 0$  or  $a = 0, b = 1$ . At every point  $x$  the basins of attraction of these two attractive fixed points are separated by an unstable fixed point at  $S = 1, Q = C(x)$  [i.e.,  $a = (1 + C)/2, b = (1 - C)/2$ ].

When  $C$  is independent of  $x$ ,  $a$  invades  $b$  if  $C < 0$  and  $b$  invades  $a$  if  $C > 0$ . In this case, when the system evolves from inhomogeneous initial conditions (for example,  $a = 0, b = 1$  for  $x > 0$  and  $a = 1, b = 0$  for  $x < 0$ ) it relaxes to the stable front solution,  $a(x) = [\tanh(x/\sqrt{2D}) + 1]/2, b(x) = 1 - a(x)$ . In this bistable model, the front admits an intrinsic width,

$$W_F = \sqrt{2D}. \quad (4)$$

Accordingly, even when the system is inhomogeneous and  $C$  is  $x$  dependent, as long as the intrinsic width of the front  $W_F$  is much smaller than the width of the transition zone  $x_t$ , the shape and the width of the front will be essentially independent of the external field, with the front location pinned to the point where  $C = 0$ , where the front velocity is zero.

The second generic scenario of pinned fronts is one that supports a transcritical bifurcation. Equation (2) fulfills this requirement, but it is a single-species model and we would like to consider the analogous two-species case. A set of PDEs that yields the required behavior is

$$\begin{aligned} \frac{\partial a(x,t)}{\partial t} &= D\nabla^2 a + a - \frac{a^2 + [1 - C(x)]ab}{K}, \\ \frac{\partial b(x,t)}{\partial t} &= D\nabla^2 b + b - \frac{b^2 + [1 + C(x)]ab}{K}. \end{aligned} \quad (5)$$

Here  $a$  and  $b$  are, again, species densities and  $C(x)$  is a background field that switches sign at  $x = 0$ . This model admits the two fixed points at  $a = K, b = 0$  and at  $a = 0, b = K$ . However, unlike the bistable case, here there is no third fixed point and for any value of  $C \neq 0$  only one fixed point is stable.

Let us say a few words about the interpretation of these models. The transcritical bifurcation model Eq. (5) describes two species that compete, say, for a common resource. If only one of the species is present, it will grow logistically until its density saturates at the carrying capacity  $K$ . The interspecific interaction term  $[1 \pm C(x)]ab$  tells us how much stress the population of one species puts on the other. If  $C$  is positive, it implies that  $b$  suffers from  $a$  more than  $a$  suffers from  $b$  (e.g., when two individuals are competing for one unit of a limiting resource,  $a$  individual has a better chance to win), so  $a$  selects out  $b$  and reaches the carrying capacity  $K$ ; the opposite is true when  $C$  is negative.

Bistable dynamics, on the other hand, is a result of a *positive feedback*. Both in Eqs. (1) and (3) the per-capita growth rate of a species is a nonlinear function of its density, meaning that (in a certain range of abundances) the fitness of a species grows with its local abundance. Accordingly, the external parameters like  $C$  do not necessarily dictate a winner: a species may compensate for negative effects of the local field by having high density, and this phenomenon explains why the system supports alternative steady states, hysteresis, etc.

The differences between these two models are most notable at the transition point. Under a transcritical bifurcation dynamics the transition occurs at  $C = 0$ , where the system supports a marginally stable manifold [every point on the line  $b = K - a$  is a stable solution of Eq. (3)]. Accordingly, at the transition the system is governed solely by noise and it moves without restrictions along this marginal line (neutral dynamics). Since this system admits no positive feedback, it also has no surface tension; therefore, in a spatial system at  $C = 0$  diffusion will completely mix the two species, i.e., the intrinsic width of the front (the analog of  $W_F$  in bistable systems) is infinite.

Under bistable dynamics, on the other hand, when the environmental conditions give no preference to one of the species ( $C = 0$ ), the most abundant species wins. Under disturbances the system may switch from one stable fixed point

to the other, but (as long as the noise is not too large and does not wash out the deterministic dynamics) these transitions will be relatively rare and the system spends most of its time close to one of the locally stable fixed points. Since the positive feedback implies positive surface tension, a spatial system will undergo a coarsening dynamics and the fronts between  $a$ -dominated and  $b$ -dominated regions are of width  $W_F$ .

### III. STATIC PROPERTIES OF THE FRONT

In this section we solve for the steady-state solutions of both models in the absence of noise, checking if one may infer the underlying dynamics from the shape of the front. The distinction between single species and competitive fronts is irrelevant to these static features (see Sec. IV), so we mainly use the single-species equations.

Let us start with the transcritical bifurcation system Eq. (5), where  $C(x) = \tanh(x/x_t)$ . As mentioned, when  $C(x) > 0$ , the fixed point (FP) of the local dynamics is  $a = K$ ,  $b = 0$ , while if  $C(x) < 0$  the FP is  $a = 0$ ,  $b = K$ . The diffusion term, however, couples the left and the right regions, so the density of each species must be a smooth function of  $x$  that approaches the FPs at large  $|x|$  and takes the symmetric value  $a = b = 1/2$  at the crossing point. For this model there is no intrinsic front width, so  $x_t$ , the width of the transition zone, sets a limit to the extent of spatial modulations. Since we are interested in the static properties of the front, there is no need to consider two different fields, and a single-field approximation is appropriate. Plugging  $b = K - a$  into Eq. (5) and setting from now on  $K = 1$ , one finds in the deterministic limit an expression which is equivalent to Eq. (2),

$$\frac{da}{dt} = D\nabla^2 a + C(x)a(1-a). \quad (6)$$

We see that the front deterministic dynamics satisfies a spatial logistic growth equation with growth rate that increases linearly in space and switches sign at the origin. A similar equation describes a deterministic, spatial voter model with selection [10], where the value of  $C$  determines the selective preference toward one of the ‘‘alleles’’ (opinions, species).

Since  $C(x)$  for  $|x| \ll x_t$  (absolute value of  $x$ ) takes a linear form, the equation for the stable front can be approximated for large  $x_t$  as

$$a''(y) + ya(y)[1 - a(y)] = 0, \quad (7)$$

where we used the dimensionless parameter  $y \equiv x(Dx_t)^{-1/3}$  and spatial derivatives are taken with respect to  $y$ . Accordingly, the front width must scale like  $[Dx_t]^{1/3}$  (note that the timescale, which reflects the inverse birth rate, was set to one).

A quite different front-width scaling was obtained in the bistable system; see Eq. (6). As explained above, in that case as long as  $W_F \ll x_t$ , the width of the transition zone plays no role and the front takes its intrinsic width  $W_F \sim \sqrt{D}$ . These differences in scaling are depicted in the lower panels of Fig. 1: the bistable front is  $x_t$  independent and its width scales with  $D^{1/2}$ , while the front width in the bifurcation model has the exponent  $1/3$  in both parameters.

Can we use these scaling differences in order to infer the underlying process from the static shape of the front? We believe that the answer, in most practical cases, is negative.

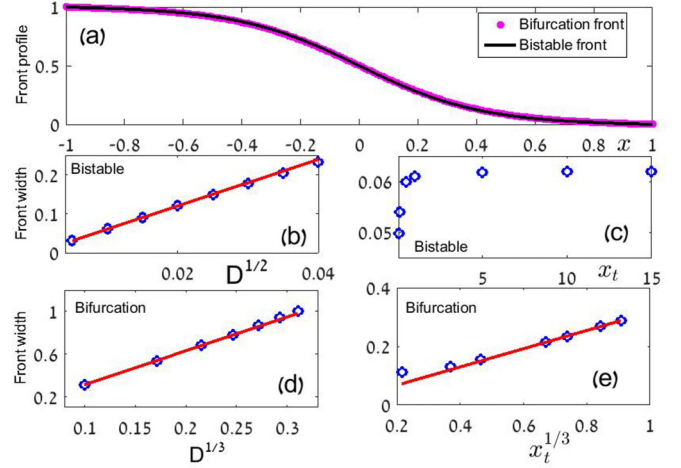


FIG. 1. The static properties of deterministic fronts: panel (a) shows both static front profiles,  $a_0(x)$  (pink, wider) and  $\phi_0(x)$  (black line), for  $D = 0.4$  and  $x_t = 0.5$ . Clearly there is no essential difference between the two. In panel (b) the width of the bifurcation front was plotted against  $D^{1/2}$  (for fixed  $x_t = 1$ , results are open circles, red line is a linear fit), and in panel (c) the same quantity is plotted against  $x_t$  for fixed  $D = 10^{-4}$ ; as predicted, the bistable front width is linear in the square root of  $D$  and is independent of  $x_t$  for when  $x_t$  is larger than the natural width of the front  $W_F$ . Panels (d) and (e) show the same relations for a bifurcation front ( $D$  varies for  $x_t = 1$ ,  $x_t$  varies for  $D = 10^{-3}$ ), demonstrating the  $(Dx_t)^{1/3}$  scaling.

If one can manipulate the diffusion constant or the width of the transition zone, the diagnosis is trivial due to the different scaling, but in most realistic cases it will be very difficult to manipulate these parameters. In principle the shape of the front might serve as an indicator, but it turns out, unfortunately, that the shapes of bifurcation and bistable fronts are very similar.

To understand that, let us return to the single-species equation for the bistable system, Eq. (1), and to its stable front solution [replacing the explicit form of  $C(x)$  by antiperiodic boundary conditions]  $\phi_0 = [\tanh(x/\sqrt{2D}) + 1]/2$ . Keeping the leading terms for small  $x$ ,  $\phi_0 \equiv 1/2 + x/\sqrt{8D}$ , one finds that the front satisfies, to first order in  $x$  and  $\phi$ ,

$$D\nabla^2 \phi(x) + (x/\sqrt{8D})\phi(x)[1 - \phi(x)] = 0. \quad (8)$$

This equation is equivalent, up to a change of scale, to the bifurcation front solution of Eq. (7), so the differences between  $\phi_0(x)$  and the solution of Eq. (7) [denoted hereon as  $a_0(x)$ ] are extremely small, as demonstrated in Fig. 1. Without measuring or varying the diffusion constant or the gradient, or monitoring the front profile to a very high degree of accuracy, one cannot use static properties to distinguish between the two possible scenarios.

### IV. NOISE, FLUCTUATIONS, AND NEGATIVE CORRELATIONS

As mentioned in the Introduction, fronts may be competitive or abiotic, meaning that the range limit of a species may be governed by an external field alone or by the competition with another species with a relative fitness that depends on the external field. For the analysis of a static front this distinction

is irrelevant: as long as the overall population  $a(x) + b(x)$  is constant or almost constant one may eliminate one variable and use the single species equation as in Sec. III. The analysis of fluctuations, on the other hand, is different, since one should understand how fluctuations of one species affect the other. The next parts of this paper are focused on competitive fronts. Before entering the calculations we would like, in this section, to clarify the alternative situations and to discuss briefly the relevance of fluctuations and correlations analysis in these cases. The considerations presented in this section are general and qualitative, since the noncompetitive fronts may respond to external and internal noise in many different ways.

Extending the basic argument presented in the Introduction, fronts may be either abiotic, competitive, or mixed. Perhaps the simplest way to clarify this classification is to consider a hypothetical removal experiment. If species A is found at  $x > 0$  and B populates the region  $x < 0$ , one may (as in the classical experiment of Connell [11]) remove one of the species and observe the resulting dynamics. If the range limits are set solely by abiotic environmental conditions, A cannot invade the negative  $x$  region even when B is removed and the same is true for B. In competitive fronts, on the other hand, the abiotic field  $C(x)$  acts indirectly, by allowing A to win in the  $x > 0$  region while B wins if  $x < 0$ , meaning that in the absence of one species its competitor may invade and capture the vacancy. Finally, as was found in Ref. [11], for example, fronts may be mixed, i.e., species A cannot invade the B region even after removal of B, meaning that its limits are purely abiotic, while B cannot invade only due to the presence of its competitor A. In Sec. III we have considered the static properties of the fronts, for which this differentiation is irrelevant. However, under noise these types of fronts may yield different results.

Living systems are usually under quite strong noise that comes from different origins. Commonly one makes a distinction between the intrinsic, demographic noise due to the stochasticity involved in the birth-death-migration process, resulting from the discreteness of the reactants, and environmental noise that reflects the fluctuations of the environment [12]. In what follows we will need another distinction, between environmental fluctuations of the controlling abiotic parameter  $C$  and other stochastic effects.

In competitive fronts the situation is relatively simple: independent of its origin, every fluctuation that harms A facilitates B and vice versa, so the densities of A and B must be negatively correlated. The anticorrelation takes its maximum value at the transition point  $x = 0$ , where the number of elementary interactions between A and B individuals, roughly proportional to  $a(x)b(x)$ , is maximal. This feature is demonstrated in Fig. 2, for both the bifurcation and the bistable scenario.

Things are more complicated, and less universal, when the front is abiotic or mixed.

First, it appears that a purely abiotic front between two species is quite a nongeneric situation. If the two species are affected by completely different external fields (say, one cannot live where the temperature is too high, the other cannot live below a certain precipitation level), the chance that their range limit coincides is tiny. Even if both species are affected by the same parameter, without the effect of competition the range limits, again, should not be at the same point. Accordingly,

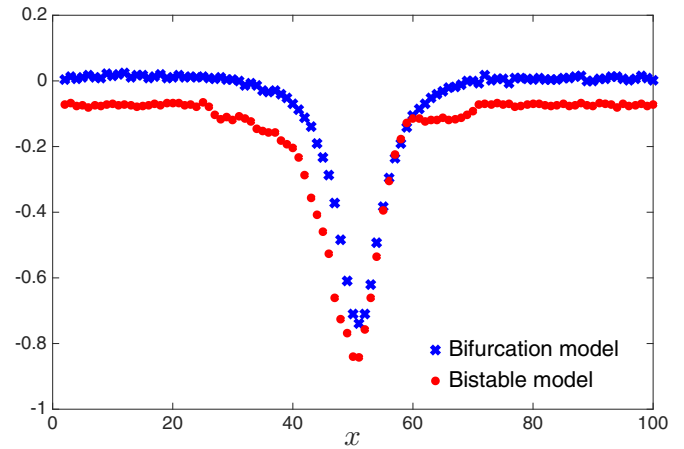


FIG. 2. The correlation between two time series,  $a(x,t)$  and  $b(x,t)$ , for a fixed distance  $x$  from the crossing point, is plotted against  $x$  for both bifurcation model (blue  $\times$ ) and the bistable model (red circles). In both models the anticorrelations between fluctuations of  $a$  and  $b$  are peaked at  $x = 0$ . Equations (3) and (5) were simulated with additional white noise that was implied independently to each of the species  $a$  and  $b$ . Results were obtained with  $D = 1/2$  and noise amplitude 0.04. For the bifurcation model  $x_t = 10$ , for the bistable model, since the front width is independent of  $x_t$ , we used antiperiodic boundary conditions.

when there is a well-defined front between two species, one should expect that it is either competitive or mixed.

For a purely abiotic front, in the simplest case of a purely abiotic front the two species do not interact with each other, there are no correlations at all. However, if the limit of both species is set by the same external parameter and if *this* parameter is fluctuating (for example, the line indicating average temperature  $T$  is moving in time) then one expects, again, negative correlations between species, as A invades the region abandoned by B and vice versa.

Still, it seems that in most cases one may use a few ad hoc indicators to clarify the situation. For example, if the colonization rate (Fisher or GL velocity, which is small close to the front) is much slower than the death rate, the peak of the anticorrelation function will appear with a lag, reflecting the time needed to the beneficiary species to realize its profits. Similar ideas may be relevant to mixed fronts, where (as long as the fluctuations are not in the control field  $C$ ) species A affects B but B does not affect A.

## V. FLUCTUATIONS STATISTICS

As demonstrated in Fig. 2, the two scenarios of competitive fronts, the transcritical bifurcation and the bistable, both yield negative correlations that takes their maximum at the crossing point. To suggest a procedure that will allow one to discriminate between them using simple and qualitative differences, let us examine the properties of the noisy system more deeply.

First, in Fig. 3 the instantaneous values of the fields are shown in the  $ab$  plane. As emphasized above, the two-species systems analyzed here [Eqs. (5) and (3)] are effectively reduced, close to the front, to the single species Eqs. (1)

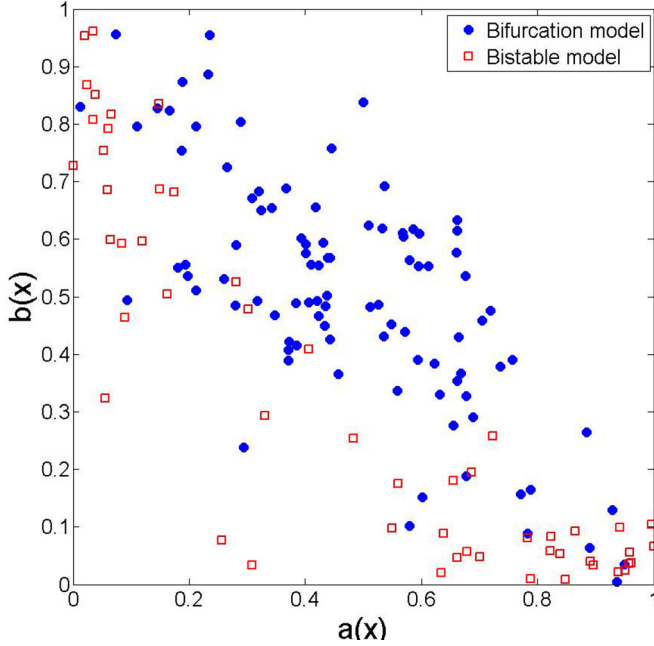


FIG. 3. A scatter plot of the instantaneous fields at different times is presented in the  $a$ - $b$  plane (without fluctuations there should be one point at  $1/2, 1/2$ ). Points from the bistable model are represented by open red squares, bifurcation model points are filled, blue circles. Fast ( $a + b$ ) and slow ( $a - b$ ) manifolds are clearly seen. Simulation parameters are identical with those of Fig. 2.

and (2). This reduction manifests itself in the appearance of slow ( $a - b$ ) and fast ( $a + b$ ) manifolds in both scenarios.

However, the sharp-eyed observer may notice a subtle qualitative difference between the two scatter plots of fluctuation amplitudes. In the bifurcation model simulations, the points appear to have higher density in the middle (around  $[0.5, 0.5]$ ), which is the steady-state value of the front at the crossing point), while the simulation of the bistable model yields a higher concentration of fluctuation points close to the two extremes  $a = 0, b = 1$  and  $a = 1, b = 0$ . This feature provides a crucial hint: the two mechanisms, bifurcation and bistability, admit qualitatively different fluctuation statistics. In the bistable scenario the noise causes the front to move quite freely (if  $x_t \gg W_F$ ) back and forth around the crossing point, so at  $x = 0$  the system is almost always either in the  $a = 1$  state or the  $a = 0$  state, leading to a fluctuation spectrum with two peaks at 0 and 1 and a dip at  $1/2$ . The bifurcation mechanism, on the other hand, yields only a single peak around the steady state value  $a(x = 0) = b(x = 0) = 1/2$ .

To quantify this, we consider first the fluctuations around the steady state front of the bifurcation model. Close to the transition point  $a(x) = a_0(x) + \delta(x, t)$ , where  $a_0(x)$  is the solution of Eq. (7), and the deviations are the result of the external noise. Linearizing Eq. (7) to first order in  $\delta$ , taking into account the front shape close to the crossing point,  $a_0(x) \sim 1/2 + c_1 x / (Dx_t)^{1/3}$ , where  $c_1$  is an  $\mathcal{O}(1)$  constant, and adding noise, one obtains a dynamical equation for the fluctuations of the bifurcation model:

$$\dot{\delta}(x, t) = D\nabla^2\delta(x, t) - \kappa x^2\delta(x, t) + \zeta(x, t), \quad (9)$$

where  $\kappa = c_1(D^{1/3}x_t^{4/3})^{-1}$  and  $\zeta$  is a white noise,  $\overline{\zeta(x, t)} = 0$  and  $\overline{\zeta(x, t)\zeta(x', t')} = \Delta\delta(x - x')\delta(t - t')$  (an overbar represent an average over realizations).

Since the deterministic part of Eq. (9) is the imaginary-time Schrödinger equation for a harmonic oscillator, an appropriate choice is to expand  $\delta$  in terms of  $\psi_m(x)$ , the normalized quantum harmonic oscillator wave functions,

$$\delta(x, t) = \sum \beta_m(t)\psi_m(x). \quad (10)$$

Using their orthonormality properties one obtains an ordinary differential equation for each mode,

$$\dot{\beta}_m(t) = -\Gamma_m\beta_m(t) + \eta(t), \quad (11)$$

with  $\Gamma_m = 2\sqrt{D\kappa}(m + 1/2)$  and  $\eta(t)$  is, again, white noise.

Equation (11) implies that every coefficient  $\beta_m$  is subject to an Ornstein-Uhlenbeck process and its probability distribution function is given by a Gaussian with zero mean and variance  $\Delta/\Gamma_m$ . An immediate result is that  $\delta$  itself is a zero-mean Gaussian, i.e., that the fluctuation density histogram is a Gaussian centered at  $a_0(x = 0) = 1/2$ . Indeed, one can do even better and calculate the variance of this Gaussian,

$$\begin{aligned} \text{Var}(\delta) &= \sum_{m \text{ even}} \psi_m^2(0)\text{Var}(\Gamma_m) \\ &= \frac{\Delta}{2\sqrt{\pi}c_1^{3/8}}\sqrt{\frac{x_t}{D}} \sum_{m \text{ even}} \frac{((m-1)!)^2}{m!(m+1/2)} \\ &= \frac{\Delta\Gamma(5/4)}{\Gamma(3/4)c_1^{3/8}}\sqrt{\frac{x_t}{D}}. \end{aligned} \quad (12)$$

In a bistable system the situation is completely different. As long as  $x_t$  is significantly larger than the internal width of the front, one can replace the external field (with exponentially small corrections in a finite system) by antiparallel boundary conditions at  $\pm\infty$ , and the fluctuations admit a zero (Goldstone) mode since the location of the front is translationally invariant. Accordingly, one finds the crossing point either in the  $a$  phase or in the  $b$  phase, with fluctuations due to the effect of noise on any of these phases. As a result, the histogram of fluctuations amplitude, instead of being a Gaussian around  $1/2$ , has two peaks that correspond to the two attractive fixed points of the homogenous problem. These features are demonstrated in Fig. 4, where the strong qualitative difference, allowing for easy discrimination between the two scenarios, is manifest.

Clearly, when  $x_t$  is much smaller than the natural width of the front, even the bistable system loses its translational invariance property, the front is trapped by the external field and cannot change significantly its spatial location, and the resulting fluctuation spectrum is peaked at  $1/2$ . In such a case we cannot offer a simple method to distinguish between the two alternative mechanisms.

## VI. EQUILIBRIUM AND OUT-OF-EQUILIBRIUM BISTABLE FRONTS

Our bistable models, Eqs. (1) and (3), describe a physical system that admits a Lyapunov function or Hamiltonian, and may be analyzed using the standard tools of statistical physics.

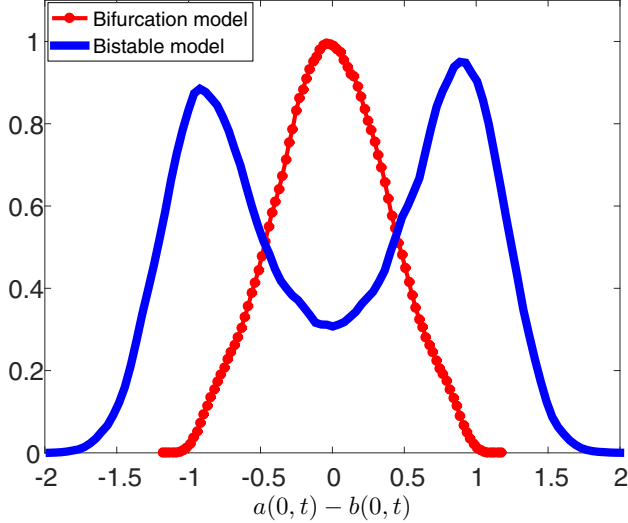


FIG. 4. Fluctuations statistics: a histogram (unnormalized) of  $a(t) - b(t)$  values at the crossing point for the bifurcation (red, filled circles) and bistable (blue line) models. In both cases noise leads to deviations from the steady-state value  $a - b = 0$ ; however, in the bifurcation case these deviations are distributed normally around the average while the bistable system distribution is bimodal. Simulation parameters are identical to those specified in the caption of Fig. 2.

To clarify the features of a pinned front in this model, we would like to stress the difference between two possible definitions of a front separating two phases.

The analysis that followed Eq. (3) regards the *instantaneous* shape of a front, i.e., the typical shape of a snapshot of the crossover region. In contrary, one may define the *time averaged*, or the “equilibrium” front, wherein the  $a$  density, say, is averaged at  $x$  over a long time span and the resulting front is the profile of  $\langle a(x) \rangle$ , where  $\langle \dots \rangle$  represents the time, or equivalently the thermodynamic, average.

The width of an equilibrium front under smoothly varying external field was analyzed recently by Ref. [3] who considered a two-dimensional  $q$ -state Potts model. These authors found that for  $q \geq 4$ , when the system has a first-order transition, the width of the front  $\langle a(x) \rangle$  scales as  $x_t^{1/3}$ , as opposed to the instantaneous front, analyzed in this paper, where the front width is independent of  $x_t$ .

To understand and generalize the results of Ref. [3], let us consider an equilibrium system at the transition point. Starting from a homogenous  $A$  state,  $B$  phase droplets with the same bulk energy are nucleated and shrink only due to the surface tension, since at the melting point there are no differences in bulk free energy. As a result, the larger the droplet, the more stable it is; monitoring the phase at a certain point  $x$  for a long time one finds  $\langle a(x) \rangle = 1/2$ , independent of the location of the measurement. Considering a randomly moving front, like the one described above, one arrives at the same conclusion.

What limits the size of these droplets, hence determining the width of the equilibrium front, is the external field gradient. If phase  $A$  invades the region  $x > 0$  (where phase  $B$  is preferred) as a compact semispherical bulge of radius  $R$ , the bulk energy

cost  $U$  of such a droplet is

$$U \propto \int_0^R (R^2 - x^2)^{\frac{d-1}{2}} \frac{x}{x_t} dx \sim \frac{R^{d+1}}{x_t}, \quad (13)$$

meaning that the width of the equilibrium front scales like  $x_t^{1/(d+1)}$ . Considering  $d = 2$ , one finds the  $x_t^{1/3}$  scaling suggested in Ref. [3]. Accordingly, the width of an equilibrium front does depend on  $x_t$ , as opposed to the width of the instantaneous front. In any case, the hallmark of a bistable system is the double peak of the fluctuation spectrum, not the shape of the front.

## VII. DISCUSSION

The problem considered here, a front pinned by smooth spatial gradient of an external field, appears to be quite generic. Especially in developmental biology and ecology, the identification of the front type may be very important, and in what follows we will try to provide some examples and references to recent literature.

The distinction between competitive and purely abiotic fronts, or in general the identification of the factors that control species range limit and stabilize its edge, is important to community ecology, both by itself and as part of the effort to understand the role of competition in natural communities (see, for example, Ref. [13], Ch. 8).

In parallel, during the past 15 years, systems that support two or more steady states, and allow for first-order transitions and catastrophic shift, became a central topic in the study of ecosystems, largely because of the concern about global environmental changes and their consequences [7,14]. Spatial effects and the impact of disturbances were considered, theoretically and experimentally, by many authors [8,15,16].

As stressed above, discontinuous transitions and catastrophic shifts are characteristics of systems with positive feedback, and allow, naturally, for alternative steady states and hysteresis loops. Demographic noise, when superimposed on the effects of an absorbing state (local extinction), acts to increase the importance of negative feedback: the strength of demographic noise is proportional to the number of individuals allowed per site, and when this number is small an increase in the density affects negatively the growth rate. Accordingly, in one-dimensional systems with demographic noise (i.e., almost any biosystem) there is no adiabatic discontinuous transition [9], while in two-dimensional systems positive feedback wins if the noise is weak but the transition becomes continuous under strong noise [6]. As showed here, the features of a pinned front may clarify the factors that govern the underlying dynamics.

A specific work that exemplifies some of the ideas considered here was published by Hirota *et al.* [4]. This work examines global vegetation patterns, classifying them into three categories: forests, savanna, and treeless. Plotting the chance of a region to be in one of these three states, the mean annual precipitation was suggested as the spatially heterogeneous field, parallel to our  $C(x)$ . These authors did not consider the possibility of a transcritical bifurcation front, and they did not have time series that allow for a direct analysis of fluctuation statistics. However, they did have statistics of many patches at the transition zone, and by plotting the relevant

histogram they indeed show a double peak at the transition line (Fig. 1 of Ref. [4]).

In a completely different field, Krotov *et al.* [5] suggested the transcritical bifurcation scenario as the underlying mechanism behind one of the most fundamental and universal aspects of developmental biology, embryonic morphogenesis. Measuring the expression levels of gap genes along the anterior-posterior axis of *Drosophila* embryos, they found strong negative correlations between spatial expression levels of gene pairs. Although they, too, did not have real time series, they implemented a technique similar to the one used in Ref. [4], interpreting the expression level at the same location in different embryos as reflecting local fluctuations.

Krotov *et al.* considered their findings as evidence for a transcritical bifurcation competitive front, and even suggested a stronger hypothesis, namely that the *entire* system, along its entire length, is at criticality, with a Goldstone mode that rotates along the anterior-posterior axis. Although their interpretation of the results appears to be supported from their analysis of spatial correlations, we believe that a simpler explanation, along the lines suggested in this paper, may also account for these observations. Moreover, their histogram of fluctuations amplitude (Fig. 3(C) of Ref. [5]), although quite noisy, appears to suggest a double-peak structure, meaning that the underlying dynamics is perhaps bistable, not bifurcational, as was already assumed for the same system in Ref. [17].

We hope to provide a careful analysis of these result in a subsequent publication.

Beyond these issues, our findings may be relevant to the effects of environmental gradient on the genetic heterozygosity of a population (see, for example, a model of competitive selection in heterogeneous environment in Ref. [18], and the data analysis presented in Ref. [19]) and on the species richness, gene transfer, and speciation in ecological communities along such a gradient (known as an ecotone or ecocline) in Refs. [20,21]. In particular, the distinction between a stable, bifurcational front and the wandering front characterizing a bistable scenario may be very relevant to the rate of gene flow and to the chance of ecotonal species to survive. Further studies of these phenomena, and in particular an appropriate characterization of fronts using fluctuation statistics, may shed new light on many fundamental processes both in physics and in the life sciences.

#### ACKNOWLEDGMENTS

We thank Herbert Levine, Michael Kalyuzhny, and Niv de-Malach for helpful discussions. N.M.S. acknowledges the support of the Israel Science Foundation, Grant No. 1427/15. D.A.K. acknowledges the support of the Israel Science Foundation, Grant No. 376/12.

- 
- [1] D. A. Kessler, Z. Ner, and L. M. Sander, *Phys. Rev. E* **58**, 107 (1998).
  - [2] W. van Saarloos, *Phys. Rep.* **386**, 29 (2003).
  - [3] C. Bonati, M. D'Elia, and E. Vicari, *Phys. Rev. E* **89**, 062132 (2014).
  - [4] M. Hirota, M. Holmgren, E. H. Van Nes, and M. Scheffer, *Science* **334**, 232 (2011).
  - [5] D. Krotov, J. O. Dubuis, T. Gregor, and W. Bialek, *Proc. Natl. Acad. Sci. USA* **111**, 3683 (2014).
  - [6] P. V. Martín, J. A. Bonachela, S. A. Levin, and M. A. Muñoz, *Proc. Natl. Acad. Sci. USA* **112**, E1828 (2015).
  - [7] M. Scheffer, S. Carpenter, J. A. Foley, C. Folke, and B. Walker, *Nature* **413**, 591 (2001).
  - [8] G. Bel, A. Hagberg, and E. Meron, *Theor. Ecol.* **5**, 591 (2012).
  - [9] H. Weissmann and N. M. Shnerb, *Europhys. Lett.* **106**, 28004 (2014).
  - [10] K. Korolev, M. Avlund, O. Hallatschek, and D. R. Nelson, *Rev. Mod. Phys.* **82**, 1691 (2010).
  - [11] J. H. Connell, *Ecology* **42**, 710 (1961).
  - [12] M. Kalyuzhny, E. Seri, R. Chocron, C. H. Flather, R. Kadmon, and N. M. Shnerb, *Am. Nat.* **184**, 439 (2014).
  - [13] G. G. Mittelbach, *Community Ecology* (Sinauer Associates, Sunderland, MA, 2012).
  - [14] S. R. Carpenter *et al.*, *Science* **332**, 1079 (2011).
  - [15] R. Durrett and S. Levin, *Theoret. Populat. Biol.* **46**, 363 (1994).
  - [16] L. Dai, K. S. Korolev, and J. Gore, *Nature* **496**, 355 (2013).
  - [17] S. Rulands, B. Klünder, and E. Frey, *Phys. Rev. Lett.* **110**, 038102 (2013).
  - [18] D. Marshall, K. Monro, M. Bode, M. Keough, and S. Swearer, *Ecol. Lett.* **13**, 128 (2010).
  - [19] G. B. Nanninga, P. Saenz-Agudelo, A. Manica, and M. L. Berumen, *Mol. Ecol.* **23**, 591 (2014).
  - [20] T. B. Smith, R. K. Wayne, D. J. Girman, and M. W. Bruford, *Science* **276**, 1855 (1997).
  - [21] S. Kark, in *Ecological Systems* (Springer, Berlin, 2013), p. 147.